# Selective combinatorial studies on Ce and Zr promoted Cu/Zn/Pd catalysts for hydrogen production via methanol oxidative reforming

S. Schuyten* and E.E. Wolf

*Department of Chemical and Biomolecular Engineering, University of Notre Dame, Notre Dame, IN 46545, USA*

The activity and selectivity for partial oxidation of methanol to $H_2$ and $CO_2$ on Zr, Ce, promoted Cu/Zn/Pd catalysts, have been studied using a high-throughput method of screening and analysis. In this work, infrared thermography was first used as a descriptor of overall catalytic activity. Then, activity and selectivity of samples with high infrared signal were measured in a flow reactor and characterized by BET, XRD, and XPS. Catalysts promoted with 10% Zr and showed $H_2$ selectivity >95% with methanol conversion approaching 100% at ~200 °C.

**KEY WORDS:** methanol; partial oxidation; cerium; zirconium; combinatorial; hydrogen production; methanol reforming.

## 1. Introduction

The use of hydrogen as a localized energy source for fuel cell powered vehicles or small electronic devices is a topic of great interest [1]. Fuel cells are efficient, with zero point of use emissions of $NO_x$, CO, volatile organic compounds (VOCs), and particulate matter. Hydrogen can be extracted from sources including natural gas, water, biomass, or other more complex hydrocarbons [2]. Despite the numerous advantages that fuel cells provide, there are significant difficulties in practice including hydrogen transportation, storage and handling. An alternative solution to problems associated with storing molecular hydrogen involves use of hydrogen stored as a liquid hydrocarbon that can be reformed on board to facilitate production of hydrogen [3]. Methanol is an abundant commodity chemical that can be stored as a liquid at ambient temperatures and shows promise as a localized hydrogen source. Research on methanol reforming has focused on four overall catalytic methanol-reforming reactions, shown in Table 1.

The first reaction (equation 1) is the methanol decomposition reaction yielding hydrogen and CO. This reaction is likely not suitable for fuel cell use because proton exchange membrane (PEM) cells, which use precious metals for catalysts, require hydrogen feed containing less than 50 ppm CO [4] to avoid catalyst poisoning. Steam reforming (equation 2) has the highest hydrogen to carbon ratio. However, this reaction is highly endothermic, not suitable for applications where a heat source is unavailable or bursts of energy may be needed. Partial oxidation (equation 3) is exothermic,

with a higher reaction rate than steam reforming and reduced tendency to form CO [5]. Finally, combined methanol reforming (equation 4) is a combination of steam reforming and partial oxidation. This reaction offers a balance between hydrogen to carbon ratio and heat of reaction but may be more difficult to control.

In recent years, high-throughput experimentation (HTE) methods have been increasing in utilization for catalyst screening and identification. This application can lead to massive parameter space searches if all material composition and processing techniques are investigated. Our group, as well as others [6–9], took a knowledge-based approach to HTE that emphasizes previous knowledge and fundamental understanding of catalytic systems to accelerate the discovery of catalytic phenomena, without testing a prohibitively large experimental parameter space. This approach, dubbed *selective combinatorial catalysis* (SCC) has been described in detail elsewhere [10]. Starting with an exhaustive literature study, a reaction model is developed which is used to select families of materials to be studied. The selected families of materials are screening first by infrared thermography (IRT), and then the activity and selectivity of a smaller subset of samples is studied in a parallel reactor.

IRT is utilized first to determine the temperature increase of individual catalyst spots in an IR reactor. In an exothermic reaction, such as methanol partial oxidation, the more active catalysts exhibit higher temperature and emit more infrared radiation. The catalysts that showed strong activity under IRT conditions are evaluated in a parallel fixed bed flow reactor, and then the most active and selective are studied in a single flow reactor. Characterization of the most active catalysts included nitrogen BET surface area measurement, X-ray

---

* To whom correspondence should be addressed.

Table 1
Methanol reforming reactions

| Equation | Reaction | $\Delta H$(g*) | $\Delta H$(l**) | $\Delta H$(l)/$H_2$ | $H_2$/C |
|---|---|---|---|---|---|
| 1 | $CH_3OH \leftrightarrow 2H_2 + CO$ | 91 | 128 | 64 | 2 |
| 2 | $CH_3OH + H_2O \leftrightarrow 3H_2 + CO_2$ | 50 | 131 | 44 | 3 |
| 3 | $CH_3OH + 1/2O_2 \leftrightarrow 2H_2 + CO_2$ | −192 | −155 | −77 | 2 |
| 4 | $4CH_3OH + 1/2O_2 + 3H_2O \leftrightarrow 11H_2 + 4CO_2$ | −44 | 238 | 22 | 2.75 |

All heats of reaction are in kJ/mol.
*All species are gas phase.
**Includes heat of vaporization for $CH_3OH$ and $H_2O$.

diffraction (XRD), and X-ray photoelectron spectroscopy (XPS) studies.

This study focus on methanol partial oxidation, which has a reaction pathway that may involve the reactions stated in Table 1 and others, such as the water gas shift reaction. Therefore, an appropriate kinetic model must include several competing reactions. For example, Peppley et al. [11,12] when studying the steam reforming reaction kinetics showed that three reactions, including water gas shift and methanol decomposition must be considered for an accurate model. Similarly, Cubeiro et al. [13], in a study of methanol partial oxidation proposed that several reactions participate including combustion, decomposition, steam reforming, and water gas shift. Clearly, all four overall reforming reactions are closely linked, and must be considered when studying the partial oxidation reaction. The model for catalysts selection was to choose a family of materials that can promote the methanol reforming and formation reactions as well as a good methanol oxidation component.

Partial oxidation of methanol has been studied over a variety of catalyst compositions including Pd on ZnO [14], or Pd on $ZrO_2$, [13], Ni on silica [15], Cu/ZnO [16, 17], $Cu/ZnO:Al_2O_3$ [18], Cu:Zn [19], and $Cu/Zn/SiO_2$ [20]. In general, group VIII noble metals such as Pd are active in methanol reforming and have been used in steam reforming producing very low CO selectivity [21]. They reported hydrogen selectivity of 96% at a methanol conversion of 70% over a Pd catalyst supported by ZnO. However, CO selectivity was still high (>20%) under the reaction conditions. In contrast, they reported CO selectivity of less than 10% was obtained over Cu containing catalysts. These CO concentrations are still several orders of magnitude higher than what is needed for use PEM fuel cell operation. Iwasa et al. [22] reports of a trade-off between high selectivity Cu:ZnO catalysts, which deactivate at temperatures above 573 K, and group VIII to X metals, which exhibit good thermal stability, but lower selectivity. Espinosa et al. [23] reported on the mechanism for partial oxidation of methanol on Cu–ZnO catalysts. Their work showed that $Cu^0$ surface area determines the reaction rate, but indicates ZnO has an important role in the catalyst structure, leading to the choice of Zn as the other primary catalyst component for this study. Ce, Zr, and Pd were selected as promoter materials based on good performance in other published studies [24–28]. So based on the extensive literature on Cu and Cu/Zn, such materials were selected as the primary component of the catalyst library for the methanol reforming reactions because its high activity and reduced tendency for formation of CO. Addition of Ce and Zr were selected as the secondary component of the methanol reforming catalysts. On the other hand Pd is well known as a good hydrocarbon oxidation catalysts and it is used for that purpose in the three way automobile catalyst for pollution control. In addition Pd has also been reported to be active both in methanol synthesis and methanol reforming [28] so it was selected as the oxidation component of the multi-component library.

Thus the catalyst library for these experiments contains 20 catalysts that are based with sites for methanol conversion (Cu/Zn, Ce, Zr) and sites for oxidative conversion (Pd). The first 12 catalysts contain variable Cu/Zn ratio starting at 5/5 to 8/2 in three groups with 0.0%, 1.0%, and 2.0% by weight Pd. The remaining 8 catalysts have a Cu/Zn ratio fixed at 7/3, which was found to be a favorable Cu/Zn ratio during IRT tests of the first 12 catalysts. Of the remaining eight, four have varying concentrations of either Ce or Zr in weight fractions of one and two with 1% by weight Pd. Two more have Ce or Zr in weight fractions of one, without Pd. The final two have both Ce/Zr in 1/1 with and without Pd. The notation selected to designate each catalyst is aCu/bZn/cCe/dZr–ePd with a–d representing Cu/Zn mole ratio, and e % weight of Pd.

## 2. Experimental

### 2.1. Infrared thermography

The IRT experimental system has been reported in detail in previous publications [10,29,30] and will be only briefly described here. The IRT reactor measures the *in situ* catalytic activity of up to 50 catalyst compositions depending on the reactor size utilized. The camera (Thermovision 782) detects infrared radiation emitted from each catalyst sample during an exothermic reaction with a precession capable of discerning 0.1 °C

temperature differences. Relative catalytic activity is determined as a function of reactor temperature using careful temperature calibrations of a blank runs and background subtraction. A large excess of reactant flows over individual catalyst wells placed in an IR transparent holder and arranged in a circular array, each containing approximately 5 mg of catalyst. This study made use of a nine-well array, due to the relatively small number of catalysts studied. Nitrogen flowing at 150 cc/min flows through a saturator containing A.C.S. spectrophotometric grade 99.9% methanol (Sigma-Aldrich) maintained at 0 °C, resulting in a stream nominally containing 3.7% methanol. Pure oxygen is added to the feed stream at a rate of 2.8 cc/min, yielding an $O_2/CH_3OH$ ratio of 0.5 at atmospheric pressure. Due to the large exothermic nature of the methanol partial oxidation reaction, significant temperature differentials were detected under reaction conditions.

## 2.2. Activity and selectivity measurements

Catalysts that showed high thermal activity during IRT experimentation were studied in a parallel flow reactor and then in greater detail using a single fixed-bed tubular reactor. Extensive results from the parallel flow reactor have been reported elsewhere [31]; here we present selected results from a single fixed bed reactor. The tubular reactor is made of quartz with an internal diameter of 10.5 mm and was thermally controlled by an electric heater. Reactor temperature is monitored and controlled using a K-type thermocouple ($\pm 1$ °C) placed in the center of the catalyst bed connected to a temperature controller. Calcined catalysts were first pressed at 35 MPa (5000 psi) for 4 min. The resulting pellet was then broken and sieved to obtain a particle size between 0.6 and 1 mm. A mass of 200 mg sieved catalyst was used in each experiment supported by quartz wool inside the reactor tube. Each catalyst was reduced *in situ* by heating from room temperature at a rate of 4.5 °C/min to 300 °C and held for 3 h. Reduction took place under a pure hydrogen flow rate of 50 cc/min. Reactant flow rate in this instance was 140 cc/min of nitrogen saturated with methanol at 0 °C, resulting in a stream containing 3.7% methanol. Oxygen is also added to the reactant stream at a rate of 2.8 cc/min, yielding an $O_2/CH_3OH$ ratio of 0.5. An overall pressure of <0.5 psi was carefully maintained inside the reactor to provide constant pressure in the GC sampling system. Two gas chromatographs were connected in parallel to analyze the reactor effluent gasses. The first (Varian 3300) contained a 12′ HAYESEP Q column for separation and detection of $CO_2$, methanol, and water. The second (Varian 920) contained a 6′ molecular sieve 5A and 15′ HAYESEP D connected in series capable of separating $O_2$, $H_2$, and CO. After reduction, the flow was switched from hydrogen to nitrogen as the reactor cooled to room temperature over the course of 30 min. Product gases were measured in 12-min intervals while the catalyst bed was heated from room temperature to 300 °C over the course of 3 h.

## 2.3. Catalyst characterization

A Quantachrom Corporation Monosorb unit that utilizes a dynamic technique with a thermal conductivity (TC) cell for measuring desorption of nitrogen was used to determine BET area. A mixture of 30% nitrogen and 70% helium is used as both carrier and adsorbent gas. Catalysts analyzed in the BET were calcined and had a particle size sieved between 0.6 mm and 1 mm (except zirconia, used as a reference, which would not form a pellet). The resulting particles were precisely weighed, and out-gassed for 2 h at a temperature of 250 °C. No other pretreatment procedures were carried out before BET measurement.

Catalyst powders analyzed via XPS and XRD were pretreated by calcination only. The X-ray diffractometer was a Scintag Inc., which used Cu Kα radiation at a wavelength of 0.1540562 nm. Scanning parameters included $2\theta$ scans from 25 to 60 degrees with a step size of 0.02 degrees and a 3 s dwell time. XPS was done using a Kratos XSAM 800 with a monochromatic Al Kα X-ray source operating at 1486.6 eV and a take-off angle fixed at 90 degrees. The powder samples were adhered to the sample stubs with conductive carbon tape and placed in a vacuum chamber with pressure lower than $2 \times 10^{-8}$ torr.

## 2.4. Catalyst preparation

Catalysts were prepared via the co-precipitation method using soluble metal precursors. In this case, nitrates of Cu, Zn, Ce, and Zr weighed in proper fractions to yield a 0.1 M total metal ion concentration in solution after being added to water. Pd nitrate was added on a weight percent basis of the other metal oxides. The nitrates were allowed to dissolve over the course of one hour while being heated to 40 °C and stirred at 400 rpm. Heating and stirring conditions were maintained while 50 mL of 0.5 M $Na_2CO_3$ is added at a rate of 1 mL per minute to precipitate the metal from aqueous solution. The resulting slurry was aged for 30 min. Next, the precipitate was filtered and thoroughly washed to minimize residual Na ions, followed by drying at 100 °C overnight. Finally, the catalyst was ground into a fine powder using a mortar and calcined in air at 500 °C for 5 h.

## 3. Results and discussion

### 3.1. Catalyst characterization

Calcined catalysts were analyzed via BET, XPS, and XRD as described previously. Results from these experiments including BET area, Cu:M ratio on the

catalyst surface, and resulting bulk concentration of metal, are summarized in table 2.

Total surface area as measured by BET is low for the Cu/Zn catalysts starting at 16 m$^2$/g for the 7Cu/3Zn–1Pd catalyst and increasing by addition of Ce, or Zr to 81 m$^2$/g in the 7Cu/3Zn/1Ce/1Zr catalyst. Addition of Zr seems to increase the surface area by a greater amount than Ce. As shown by XPS, this is not surprising since Zr enriches Cu on the surface more than Ce.

XRD patterns of the calcined samples (not shown) indicate distinct separate oxide phases of the catalytic components prior to reduction and reaction. Xi *et al.* [32] reported change from oxide phases to metallic upon reduction in hydrogen, and formation of Cu/Zn alloys under reduction in CO or during methanol decomposition reaction conditions. Mole % bulk compositions obtained from XRD results presented in table 2, show a higher concentration of Cu when Ce or Zr are added, roughly 15–20% relative to concentration initially present in solution. This could be due to a decrease in the solubility of Zn during preparation due to the presence of Ce or Zr nitrates resulting in enrichment of Cu in the precipitated solid. Due to its low concentration, XRD results did not reveal any peaks that could be attributed to Pd, thus it was not taken into account for the XRD analysis.

XPS results show Zn in a much higher proportion on the surface by a factor of three or more, when compared to the bulk. Catalyst samples containing Zr made impossible the quantification of Pd peaks by XPS because the Pd 3d doublet overlaps with the intense Zr 3p peak. XPS results show a significant enrichment of Pd on the surface when Ce is added, from Cu/Pd of 250 to 1.4.

## 3.2. Infrared thermography

All 20 prepared catalysts described previously were evaluated by IRT in 3 experiments, each array containing up to 9 catalysts including references samples for calibration. A $\Delta T$ observed for each catalyst spot before and during reaction, at two reactor temperatures of 225 and 250 °C. Due to the large exothermic nature of the

partial oxidation of methanol reaction, (−192 kJ/mol of CH$_3$OH reacted) the active catalysts exhibited a large, easily observed, $\Delta T$. Results from the IRT experiments are presented for all 20 catalysts in figures 1 and 2. The smallest $\Delta T$ observed during the IRT experiments was 2 °C, still easily detectable by the IR camera, which has 0.1 °C precision capability. All catalysts except for one (7Cu/3Zn/1Zr–1Pd) showed a trend of increasing $\Delta T$ with increasing reactor temperature from 225 °C to 250 °C.

Figure 1 displays results for 12 catalysts, showing the effect of changing four values of the Cu/Zn ratio from 5/5 to 8/2, and the effect of adding Pd metal in 0.0%, 1.0%, and 2.0% (weight percent relative to metal oxides) to each of those. Clearly, increasing the Cu:Zn ratio increases $\Delta T$, regardless of Pd metal loading. The increase is roughly 5 °C between 5Cu/5Zn and 8Cu/2Zn catalysts, for all three Pd metal loadings, at both reactor temperatures. The addition of 1% Pd metal has a larger effect on the observed $\Delta T$, though changing Pd loading from 1.0% to 2.0% yields no significant change in $\Delta T$ given the same Cu/Zn ratio.

The results shown in figure 2 for eight catalysts demonstrate the effect of addition of Ce and Zr to the 7Cu/3Zn catalysts at a Pd loading of 1.0% with Ce and/or Zr added in a ratio Cu/M equal to 7/1 and 7/2. The addition of Ce or Zr, especially when combined with Pd, had a pronounced effect on $\Delta T$. Interestingly, when both Ce and Zr are added the activity enhancement was less than when a single promoter was added. Addition of 1 part of Zr yields the highest observed $\Delta T$ among all the 20 catalysts. Further addition of two parts of Zr did not significantly increase $\Delta T$. Promotion of the catalyst by Ce also yielded significant increase in $\Delta T$, with addition of two parts Ce better than just one. As shown in the unpromoted Cu/Zn catalysts, the $\Delta T$ was greatly enhanced through addition of just a small amount of Pd, except for those catalysts containing both Ce and Zr.

## 3.3. Activity and selectivity measurements

Six catalysts were selected for more detailed activity and selectivity measurements based on the performance

Table 2
Summary of data from BET/XRD/XPS

| Catalyst | Preparation mole % | | | | | BET area m$^2$/g | XPS surface molar ratio | | | | XRD Mole % | | | | |
|---|---|---|---|---|---|---|---|---|---|---|---|---|---|---|---|
| Cu/Zn/Ce/Zr–Pd | Cu | Zn | Ce | Zr | Pd* | | Cu/Zn | Cu/Ce | Cu/Zr | Cu/Pd | Cu | Zn | Ce | Zr | Pd* |
| 5/5/0/0-0 | 50 | 50 | 0 | 0 | 0 | 16 | 0.3 | – | – | – | 50 | 50 | 0 | 0 | – |
| 7/3/0/0-1 | 70 | 30 | 0 | 0 | 1 | 34 | 0.7 | – | – | 250 | 72 | 28 | 0 | 0 | – |
| 7/3/0/1-1 | 64 | 27 | 0 | 9 | 1 | 60 | 1 | – | 10 | ** | 84 | 13 | 0 | 4 | – |
| 7/3/1/0-1 | 64 | 27 | 9 | 0 | 1 | 38 | 0.8 | 5 | – | 1.4 | 77 | 19 | 4 | 0 | – |
| 7/3/1/1-0 | 58 | 25 | 8 | 8 | 0 | 81 | 0.7 | 5 | 5 | – | 80 | 10 | 7 | 3 | – |
| Ceria | 0 | 0 | 100 | 0 | 0 | 17 | – | – | – | – | – | – | – | – | – |
| Zirconia | 0 | 0 | 0 | 100 | 0 | 52 | – | – | – | – | – | – | – | – | – |

*Pd prepared on a weight percent based on metal oxides.
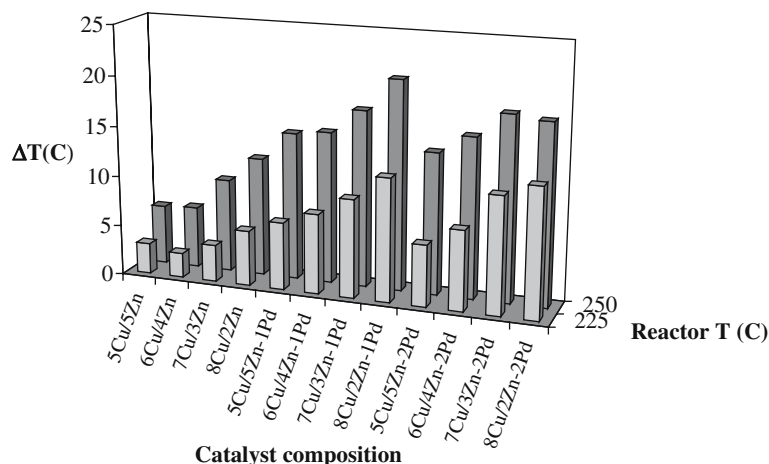**Pd peaks could not be quantified for catalysts containing Zr.

Figure 1. Plot of observed catalytic activity $\Delta T$ versus catalyst compositions; Cu/Zn ratio from 5/5 to 8/2 and Pd metal in 0.0%, 1.0%, and 2.0% (weight percent relative to metal oxides) at reactor temperatures 225 and 250 °C.

in the IRT reactor at 250 °C. The compositions studied include 7Cu/3Zn–1Pd, 7Cu/3Zn/1Zr–1Pd, 7Cu/3Zn/2Zr–1Pd, 7Cu/3Zn/1Ce–1Pd, 7Cu/3Zn/2Ce–1Pd, and 7Cu/3Zn/1Ce/1Zr–1Pd. For each experiment, 200 mg of the sieved catalyst was reduced *in situ* under hydrogen at a flow rate of 50 cc/min. Reactant flow rate in this instance was 140 cc/min of nitrogen saturated with methanol at 0 °C, resulting in a stream containing 3.7% methanol. Pure oxygen was added to the methanol–nitrogen stream at a rate of 2.7 cc/min, yielding an $O_2$/$CH_3OH$ ratio of 0.5.

The six catalysts studied attained high methanol conversion rates, as shown in figures 3 and 4, reaching 90%+ at 200 °C. Figure 3a, c shows that, in agreement with the IRT results, addition of Zr enhances conversion of the 7Cu/3Zn–Pd catalyst. Auto-ignition was seen when one part Zr was added to Cu/Zn, however, adding more Zr did not display this effect. Consumption of oxygen reached 100% for all catalysts studied at a temperature of roughly 150 °C. Agrell *et al.* [33] found a

strong dependence of conversion on the oxygen partial pressure. Our results (not shown) show a similar trend. The profiles of the most active catalysts show an S shaped curve through the temperature ramp with the less active catalysts showing a steeper middle slope. This steep slope could indicate a change in the nature of the catalyst surface which results in the same structure that is present in the more active catalysts. Shen and Song [34] reported that changing catalyst preparation has an effect on its reducibility, with CuO reduction temperature ranging from 230 to 477 °C, as measured by TPR, depending on the preparation method. A similar effect might explain the observed changes in ignition temperature.

Figure 3b, d shows the effect of Ce promotion to the Cu/Zn–Pd catalyst. In both cases the addition of Ce did not significantly increase the conversion of methanol relative to Cu/Zn–Pd. The addition of both Ce and Zr promoters (not shown) also did not improve conversion relative to the base catalyst. Hydrogen selectivity
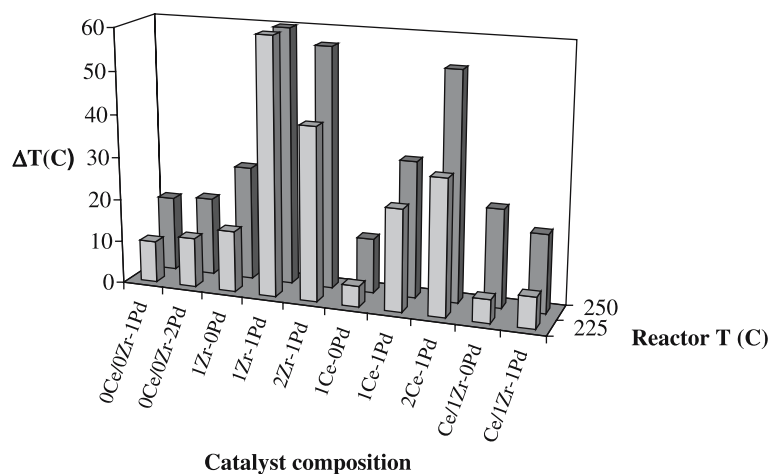


Figure 2. Plot of observed catalytic activity $\Delta T$ versus catalyst compositions; Cu:Zn fixed at 7/3 with variable additions of Ce, Zr, and Pd at reactor temperatures 25 and 250 °C.

**(a)  Methanol conversion Zr promoted**

**(b)  Methanol conversion Ce promoted**

**(c)  Hydrogen selectivity Zr promoted**

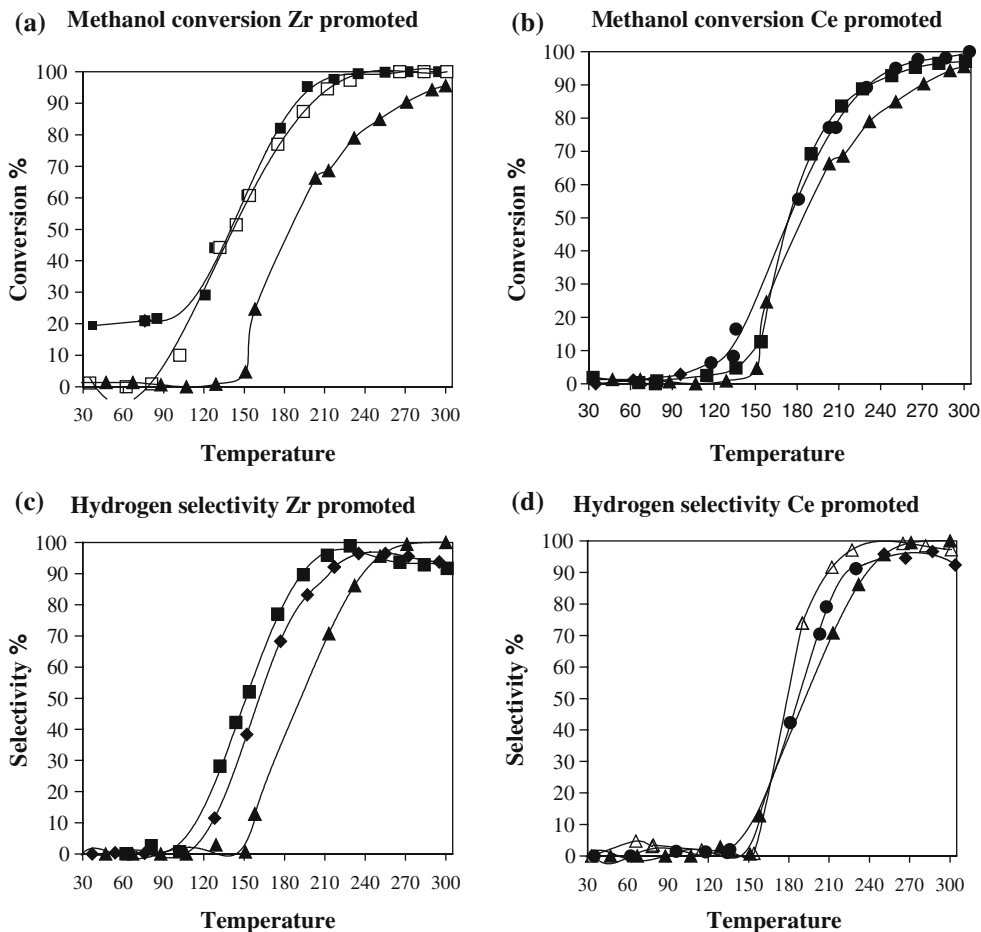**(d)  Hydrogen selectivity Ce promoted**

Figure 3.  Methanol conversion and hydrogen selectivity versus temperature showing effect of Zr and Ce promotion. Cu/Zn/Ce/Zr–Pd, (■) 7Cu/3Zn/0Ce/1Zr–1Pd, (□) 7Cu/3Zn/0Ce/2Zr–1Pd, (▲) 7Cu/3Zn/0Ce/0Zr–1Pd, (△) 7Cu/3Zn/2Ce–1Pd, (●) 7Cu/3Zn/1Ce–1Pd.

increased along with methanol conversion as reaction temperature increased before reaching a plateau when methanol conversion approached 100%. Between 250 and 300 °C, maximum hydrogen selectivity was observed to be between 99% for catalyst 7Cu/3Zn–1Pd and 96% for 7Cu/3Zn/1Ce–1Pd. Below 175 °C catalyst 7Cu/3Zn/1Zr–1Pd exhibited the highest hydrogen selectivity, it also had highest methanol conversion throughout the reaction profile.

In figure 4 the $CO_2$ selectivity has been plotted versus reaction temperature with a single trend line through the data in the upper temperature region. A significant amount of carbon dioxide and water was detected in the low temperature regions where methanol conversion is <70%. This indicates that combustion processes may be the dominant reaction at lower temperatures. The Zr promoted catalyst rapidly approaches a plateau starting at 200 °C of roughly 95% hydrogen selectivity. This result is interesting since the $CO_2$ selectivity increases much less dramatically between 100 and 200 °C, where both methanol conversion and hydrogen selectivity are rapidly increasing, possibly due to the water gas shift reaction. CO formation completes the carbon balance, yielding a concentration less than 6000 ppm for all
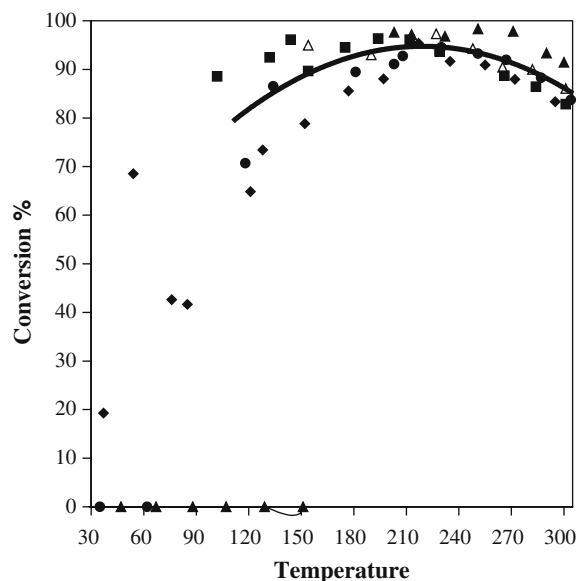
Figure 4.  Carbon dioxide selectivity plotted versus reaction temperature for catalysts: (■) 7Cu/3Zn/1Zr–1Pd, (▲) 7Cu/3Zn–1Pd, (□) 7Cu/3Zn/2Zr–1Pd, (●) 7Cu/3Zn/1Ce–1Pd, (△) 7Cu/3Zn/2Ce–1Pd.

catalysts studied. Catalyst promoted with zirconia 7Cu/3Zn/1Zr achieved 1400 ppm CO at 100% methanol conversion and 92% hydrogen selectivity.

Hydrogen selectivity versus methanol conversion is plotted in figure 5 for all the catalysts studied. A single trend line shows similar dependence of hydrogen selectivity on methanol conversion for all catalysts. Three distinct regions can be seen in this figure. In the low methanol conversion region, below approximately 20% there is almost no hydrogen formation, likely due to the reaction being dominated by complete combustion as seen by Agrell *et al.* in a study of partial oxidation over ZnO supported Pd [14]. Next in the region from 30% to 80% methanol conversion, a roughly linear dependence is seen as combustion processes yield to other reactions possibly involving methanol decomposition and water gas shift (WGS). The last region from methanol conversion 80% to 100% yields a decreasing slope, turning negative at conversion >95% as the reverse water gas shift products (increased CO and $H_2O$) begin to form. Thus an optimum operation range for all catalysts under the reaction conditions studied is ~95% conversion.

The two most active catalysts (7Cu/3Zn/1Zr–1Pd, and 7Cu/3Zn/2Zr–1Pd) correspond to the catalysts with the highest IRT signal, showing good agreement between IRT and reaction results. Data from catalyst characterization summarized in table 2 shows the addition of Ce or Zr enhances the concentration of copper on the surface relative to Zn. Active sites are reported in literature to be $Cu^0$ and/or $Pd^{\sigma+}$. Aljo *et al.* [35] using $N_2O$ adsorption–decomposition while studying partial oxidation over Cu/ZnO catalysts determined the $Cu^0$ surface area and showed catalysts with highest $Cu^0$

surface area had the highest catalytic activity. Similarly Liu *et al.* [36] reported that the more active $Pd^{\sigma+}$ was maintained by $Zr^{4+}$ ion modification due to acid sites in the support. Therefore, the high activity of the catalysts at low temperatures of 7Cu/3Zn/2Ce–1Pd, 7Cu/3Zn/1Zr–1Pd, and 7Cu/3Zn/2Zr–1Pd may be due to enhancement of Cu and/or Pd on the surface. Iwasa *et al.* [37] reported on formation of PdZn alloys under various reduction conditions and found catalysts containing such alloys were much more active and selective than those containing separate metallic phases. All these transformations might be occurring during the genesis of the most active surfaces.

Comparison of activity in terms of the rate of hydrogen production per gram of catalyst, conversion, and selectivity shows that Ce and Zr promoted catalysts are within range of other literature results for methanol reforming. The hydrogen selectivity in this study averaged approximately 95% at 100% methanol conversion, which corresponds to a production rate of ~3100 cc $H_2$/g h. Other studies utilizing catalysts containing Cu, Zn, Zr and/or Pd report catalyst performance ranging from 966 to 4700 cc/g h at 80–90% conversion and 45–82% selectivity [13,14,22,35,38].

As stated previously, there is a potential for several reactions to compete simultaneously under partial oxidation conditions, including all four overall methanol reforming reactions. When considering the results previously discussed, the dramatic change in reaction product distribution as a function of temperature agrees with previous literature results [14] in that several reaction mechanisms are competing and the dominant one is dependant upon the temperature and/or other reaction conditions. The WGS reaction may play a significant role in the reaction pathway. Further work is underway to determine its role in hydrogen selectivity.
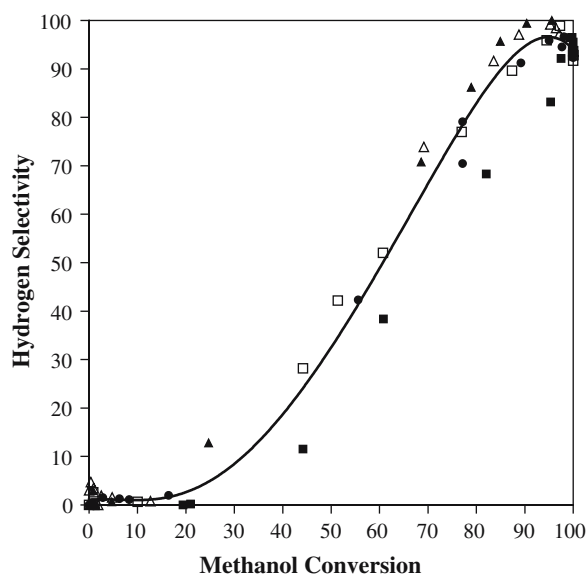
## 4. Conclusions

An initial library consisting of 20 co-precipitated catalysts containing Cu and Zn promoted with Ce, Zr, and/or Pd were shown to be both active and selective for the partial oxidation of methanol. This study represents the first time Zr and Ce have been added to Cu/Zn catalysts for study under partial oxidation conditions. However, CO selectivity was still too high (a few thousand PPM) for use in PEM fuel cells without further purification.

The library was evaluated in a two-stage HTE process. First, catalysts were evaluated based on temperature rise as a result of the exothermic reaction, detected by an infrared camera. Secondly, a more detailed activity study capable of detecting both activity and selectivity was carried out in a single flow tubular reactor. Results from these studies will form the basis for the development of the next catalytic library.



Figure 5. Hydrogen selectivity plotted versus methanol conversion for catalysts: (■) 7Cu/3Zn/1Zr–1Pd, (▲) 7Cu/3Zn–1Pd, (□) 7Cu/3Zn/2Zr–1Pd, (●) 7Cu/3Zn/1Ce–1Pd, (△) 7Cu/3Zn/2Ce–1Pd.

We found $H_2$ selectivity >95% in a catalyst promoted with Zr at 100% methanol conversion. The most active catalyst was also promoted with Zr and achieved 100% methanol conversion at 225 °C. This catalyst post-reduction auto-ignited up to a temperature of approximately 50 °C upon reactant introduction, with no external heat input or control. Further studies are under way to better characterize the catalysts and reaction mechanism including the role of Cu/Zn alloys and determine the role of each component in regards to activity and selectivity.

## Acknowledgements

## References

[1] G.J.K. Acres, J. Power Sources 100 (2001) 60.
[2] G.P. Nowell, *The Promise of Methanol Fuel Cell Vehicles* (1998).
[3] A. Kulprathipanja and J.L. Falconer, Appl. Catal. A-Gen. 261 (2004) 77.
[4] A.F. Ghenciu, Curr. Opin. Solid State Mater. Sci. 6 (2002) 389.
[5] L.F. Brown, Int. J. Hydrogen Energ. 26 (2001) 381.
[6] P.P. Pescarmona, J.C. van der Waal, I.E. Maxwell and T. Maschmeyer, Catal Lett. 63 (1999) 1.
[7] C. Hoffmann, H.W. Schmidt and F. Schuth, J. Catal. 198 (2001) 348.
[8] R.J. Berger, J. Perez-Ramirez, F. Kapteijn and J.A. Moulijn, Appl. Catal. A-Gen. 227 (2002) 321.
[9] F. Gracia, W. Li and E.E. Wolf, Catal. Lett. 91 (2003) 235.
[10] W. Li, F.J. Gracia and E.E. Wolf, Catal. Today 81 (2003) 437.
[11] B.A. Peppley, J.C. Amphlett, L.M. Kearns and R.F. Mann, Appl. Catal. A-Gen. 179 (1999) 21.
[12] B.A. Peppley, J.C. Amphlett, L.M. Kearns and R.F. Mann, Appl. Catal. A-Gen. 179 (1999) 31.
[13] M.L. Cubeiro and J.L.G. Fierro, Appl. Catal. A-Gen. 168 (1998) 307.
[14] J. Agrell, G. Germani, S.G. Jaras and M. Boutonnet, Appl. Catal. A-Gen. 242 (2003) 233.
[15] Y. Matsumura, K. Tanaka, N. Tode, T. Yazawa and M. Haruta, J. Mol. Catal. A-Chem. 152 (2000) 157.
[16] J. Agrell, M. Boutonnet, I. Melian-Cabrera and J.L.G. Fierro, Appl. Catal. A-Gen. 253 (2003) 201.
[17] J. Agrell, M. Boutonnet and J.L.G. Fierro, Appl. Catal. A-Gen. 253 (2003) 213.
[18] R.M. Navarro, M.A. Pena and J.L.G. Fierro, J. Catal. 212 (2002) 112.
[19] T.J. Huang and S.W. Wang, Appl. Catal. 24 (1986) 287.
[20] Z.F. Wang, W.P. Wang and G.X. Lu, Int. J. Hydrogen Energ. 28 (2003) 151.
[21] Y.H. Chin, R. Dagle, J.L. Hu, A.C. Dohnalkova and Y. Wang, Catal. Today 77 (2002) 79.
[22] N. Iwasa, T. Mayanagi, W. Nomura, M. Arai and N. Takezawa, Appl. Catal. A-Gen. 248 (2003) 153.
[23] L.A. Espinosa, R.M. Lago, M.A. Pena and J.L.G. Fierro, Top. Catal. 22 (2003) 245.
[24] S. Imamura, T. Hagashihara, Y. Saito, H. Aritani, H. Kanai, Y. Matsumura and N. Tsuda, Catal. Today 50 (1999) 369.
[25] M.P. Kapoor, Y. Ichihashi, K. Kuraoka, W.J. Shen and Y. Matsumura, Catal. Lett. 88 (2003) 83.
[26] M.P. Kapoor, A. Raj and Y. Matsumura, Micropor. Mesopor. Mat. 44 (2001) 565.
[27] Y.Y. Liu, T. Hayakawa, K. Suzuki and S. Hamakawa, Appl. Catal. A-Gen. 223 (2002) 137.
[28] Y. Choi and H.G. Stenger, Appl. Catal. B-Environ. 38 (2002) 259.
[29] J.C. Kellow and E.E. Wolf, Chem. Eng. Sci. 45 (1990) 2597.
[30] F.C. Moates, M. Somani, J. Annamalai, J.T. Richardson, D. Luss and R.C. Willson, Ind. Eng. Chem. Res. 35 (1996) 4801.
[31] E. Wolf, S. Schuyten and D.J. Suh, *Combinatorial and High Throughput Discovery and Optimization of Catalysts and Materials* (CRC Press, 2005, In Press).
[32] J.Y. Xi, Z.F. Wang and G.X. Lu, Appl. Catal. A-Gen. 225 (2002) 77.
[33] J. Agrell, K. Hasselbo, K. Jansson, S.G. Jaras and M. Boutonnet, Appl. Catal. A-Gen. 211 (2001) 239.
[34] J.P. Shen and C.S. Song, Catal. Today 77 (2002) 89.
[35] L. Alejo, R. Lago, M.A. Pena and J.L.G. Fierro, Appl. Catal. A-Gen. 162 (1997) 281.
[36] Y.Y. Liu, T. Hayakawa, T. Ishii, M. Kumagai, H. Yasuda, K. Suzuki, S. Hamakawa and K. Murata, Appl. Catal. A-Gen. 210 (2001) 301.
[37] N. Iwasa, S. Masuda, N. Ogawa and N. Takezawa, Appl. Catal. A-Gen. 125 (1995) 145.
[38] Z.F. Wang, J.Y. Xi, W.P. Wang and G.X. Lu, J. Mol. Catal. A-Chem. 191 (2003) 123.